Artificial dense lattice of magnetic bubbles

M. V. Sapozhnikov, S. N. Vdovichev, O. L. Ermolaeva, N. S. Gusev, A. A. Fraerman, S. A. Gusev, and Yu. V. Petrov

---

Articles you may be interested in

Edge-modulated perpendicular magnetic anisotropy in [Co/Pd] n and L10-FePt thin film wires
Appl. Phys. Lett. **107**, 182408 (2015); 10.1063/1.4935104

Controlled domain wall pinning in nanowires with perpendicular magnetic anisotropy by localized fringing fields
J. Appl. Phys. **115**, 17D506 (2014); 10.1063/1.4864737

Magnetic strip patterns induced by focused ion beam irradiation
J. Appl. Phys. **103**, 063915 (2008); 10.1063/1.2894587

Enhanced exchange bias effects in a nanopatterned system consisting of two perpendicularly coupled ferromagnets
Appl. Phys. Lett. **92**, 022508 (2008); 10.1063/1.2833124

Soft x-ray resonant magnetic scattering from an imprinted magnetic domain pattern
Appl. Phys. Lett. **89**, 092507 (2006); 10.1063/1.2344935

NEW Special Topic Sections

NOW ONLINE
Lithium Niobate Properties and Applications: Reviews of Emerging Trends

AIP | Applied Physics Reviews

Artificial dense lattice of magnetic bubbles

M. V. Sapozhnikov,[1,a] S. N. Vdovichev,[1] O. L. Ermolaeva,[1] N. S. Gusev,[1] A. A. Fraerman,[1] S. A. Gusev,[1] and Yu. V. Petrov[2]

[1]*Institute for Physics of Microstructures RAS, GSP-105, Nizhny Novgorod, Russia and N. I. Lobachevskii State University, Nizhny Novgorod 603950, Russia*
[2]*Saint Petersburg State University, Universitetskaya nab. 7/9, St. Petersburg 199034, Russia*

Co/Pt multilayers with perpendicular magnetic anisotropy are irradiated by focused He$^+$ ion beam to locally reduce the anisotropy value. The irradiated spots with a diameter of 100 nm are arranged in a square lattice with 200 nm period. The formation of the nonuniform periodic magnetic structure is observed without changes in the film topography. The spatial symmetry of the magnetic force microscopy signal and the specific shape of magnetization curves indicate the formation of the magnetic bubbles or magnetic vortices within the irradiated spot depending on the irradiation dose. The experimental data are in a good agreement with micromagnetic simulations of the system. *Published by AIP Publishing.* [http://dx.doi.org/10.1063/1.4958300]

Soliton-like solutions for magnetization of the materials with uniaxial anisotropy were found in 1970s.[1,2] Later, this topological charged solitons usually referred to as "magnetic skyrmions" were observed experimentally in chiral magnetic materials.[3–6] The rising interest to them is caused by their unusual spin-electronic properties, such as the topological Hall effect[7,8] or current-driven motion in ultralow currents,[9] which can be exploited in spintronic devices combining information storage and processing. The disadvantage is that the Dzyaloshinskii–Moriya interaction (DMI)[10–12] stabilising the magnetic skyrmion lattices in the chiral magnets is usually weak, and thus, the skyrmions can be stable only within a narrow temperature-field region[13] which hinders their application.

Nevertheless, now it becomes clear that the proper nano-structuring can help to overcome these obstacles and allows obtaining magnetic skyrmions in ordinary (without DMI) conducting magnetic materials at zero field and room temperature. The first idea is to place Co particles with vortex distribution of the magnetization on the surface of the CoPt film with the perpendicular anisotropy. It was demonstrated by numerical micromagnetic simulations[14,15] followed by experimental investigation[16–18] that in this case the skyrmions can be stabilized in the CoPt film due to the exchange interaction with the magnetic vortex. The investigated artificial skyrmion lattices have the average topological charge densities (i.e., the number of skyrmions per square micron) up to 4 μm^{-2} in the better case.[18] This is much less than the skyrmion densities in the chiral magnets. As the transport topological effects, such as topological Hall effect, are proportional to the average density of the topological charge, it is the important parameter of a system.

Another method of the magnetic film nanostructuring consisting in spatial modulation of its thickness[19] or local change of material parameters of the film[20] is recently suggested. The idea behind this method is that in this case the domain wall surrounding the skyrmion core has different energies in different regions of the film and this can prevent skyrmions from collapse or runout even in the absence of DMI. In this work, we experimentally verify the predicted[20] possibility to stabilize the topologically charged magnetic states in the common metallic ferromagnetic films by spatial modulation of the perpendicular anisotropy value. It is well known that the anisotropy coefficient of magnetic Co/Pt multilayers can be changed by He or Ga ion irradiation.[21–23] Depending on the irradiation dose, the value of the perpendicular anisotropy can be reduced or even becomes the easy-plane. In this work, the focused ion beam irradiation technique is used to fabricate lattices of the nanospots with the reduced anisotropy (we will refer them below simply as "spots" to be short) in the initially uniform magnetic Co/Pt film with the perpendicular anisotropy.

The experimental samples were fabricated by nanostructuring of the Co/Pt multilayers consisting of 5 alternating Co (0.5 nm thick) and Pt (1 nm thick) layers. The structure is grown by DC magnetron sputtering on a SiO$_2$ substrate with Ta (10 nm)/Pt (10 nm) buffer layers. The magnetization loop of the Co/Pt film measured by the magneto-optical Kerr effect shows the existence of the perpendicular magnetic anisotropy (Fig. 1(a)). Using standard UV photolithography, we fabricate a 10 μm wide microbridge from the Co/Pt film (Fig. 1(b)). The width of the probes is 2 μm. A Carl Zeiss Orion helium ion microscope equipped with a Nanomaker pattern generator is used to fabricate rectangular lattices of the irradiated spots in the area of the Hall cross. The spots have the diameter of 100 nm, and the lattice period is 200 nm (Fig. 1(c)). The irradiation is done by a raster method using the focused ion beam having 5 nm in diameter and the step of scanning of 2 nm. As a result, the irradiation is practically uniform within the area of the spot. The irradiation doses varied for different samples from 1×10^{15} to 4×10^{15} ions/cm^2, and the energy of the ions is 30 keV. The whole irradiated area is 20×14 μm.

The atomic force microscopy (AFM) investigations demonstrate that the flatness of irradiated areas is the same as the flatness of the as-prepared film. The magnetic states of

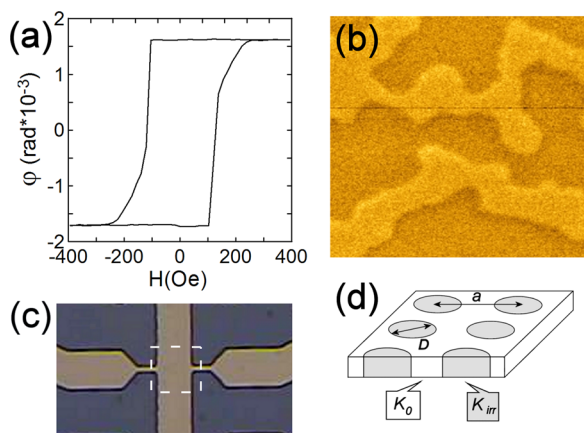a)Author to whom correspondence should be addressed. Electronic mail: msap@ipmras.ru

FIG. 1. (a) The typical view of the polar MOKE hysteresis of the initial Co/Pt superlattice. (b) The $2 \times 2 \, \mu m$ MFM image of the typical labyrinth domain structure of the initial Co/Pt superlattice. (c) The photo of the Hall bridge; the lattice is formed in the area bordered with the dashed line. (d) The geometry of nanomodification: the irradiated spots with the reduced anisotropy ($D = 50$, $100 \, nm$) form the rectangular lattice (period is 100, $200 \, nm$).

the samples are investigated by the MFM. The magnetization distributions are measured at zero external field in two states: in the remanent state after magnetizing in the high (3000 Oe) perpendicular field and in the demagnetized state. The demagnetized state is achieved after applying oppositely directed magnetic field (100–200 Oe) to the remanent state. The results of the MFM investigations are summarized here:

- The formation of the labyrinth domain structure in the demagnetized state (Fig. 2(a)) occurs in the initial Co/Pt multilayers, and the irradiation dose 1×10^{15} ions/cm^2 does not affect on the magnetic structure of the sample.
- For the doses 2–4×10^{15} ions/cm^2, the irradiated spots demonstrate individual magnetic contrast (Fig. 2). The MFM signal has the radial symmetry which indicates the radial symmetry of the magnetization distribution within the spot; we do not observe magnetic poles of the different sign within the same spot. Besides the individual spots, the large-scale domains with the different direction of the magnetization in the nonirradiated areas of the film (Figs. 2(b) and 2(d)) are observed in the demagnetized state. While the individual MFM signal of the spots is very similar for all irradiation doses, the overall picture is very different for the dose of 2×10^{15} ions/cm^2 (referred below as small dose) and for the doses of 3×10^{15} and 4×10^{15} ions/cm^2 (referred below as high doses). What is the difference?
- In the case of the high irradiation doses, all the spots demonstrate MFM signals in both the remanent (Fig. 2(a)) and the demagnetized states (Fig. 2(b)). They have the MFM contrast within the areas of both up and down perpendicularly magnetized domains in the demagnetized state (Fig. 2(b)).
- In the case of the small irradiation dose, only 75% of the spots show the MFM contrast in the remanent state while 25% of the spots have the magnetization the same as the one in the surrounding area (Fig. 2(c)). Similarly in the demagnetized state, the spots are visible only within the area of the domains with the initial orientation of the
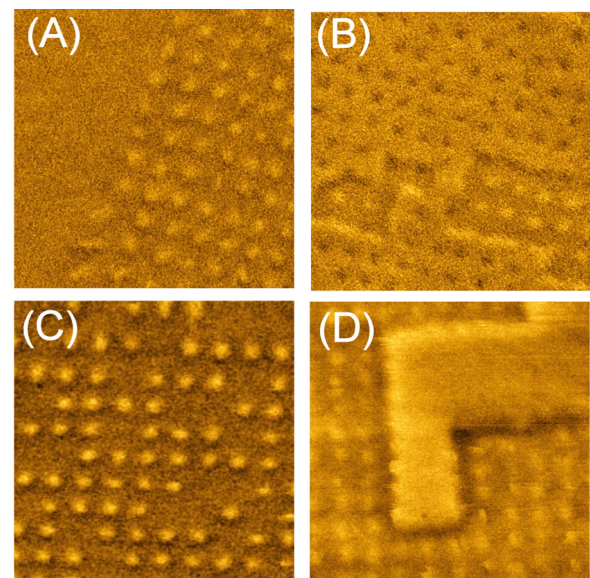

FIG. 2. The MFM images of the samples. The scan area is $2 \times 2 \, sm$. (a) and (b) The sample with $100 \, nm$ highly irradiated spots (here the dose is 4×10^{15} ions/cm^2), and the corresponding remanent and demagnetized states. The edge of the lattice is seen in (a), demonstrating the absence of the domains in the initial Co/Pt superlattice in the remanent state. In the demagnetized state (b), the domains with the both magnetization direction contains the spots with MFM contrast. (c) and (d) The sample with $100 \, nm$ spots irradiated with the dose of 2×10^{15} ions/cm^2, and the corresponding remanent and demagnetized states. The degree of the spots demonstrating MFM contrast is 75% in the remanent state in this case. In the demagnetized state, the domain with the initial direction of the magnetization contains the spots, while the domain with the reversed magnetization does not demonstrate any inner MFM contrast.

magnetization (Fig. 2(d)), and the domains with the reversed magnetization do not have the spots showing the MFM contrast.

We also measured the hysteresis curves of the Hall effect in our samples represented in Fig. 4. What are the specific features of the curves which need to be addressed? The remanent Hall signal for the sample with the small irradiation dose (Fig. 4(a)) is practically equal to the saturation value (97%). The case of the both high irradiation doses is different. In the latter case: (1) The remanent Hall signal is 80% of the saturation. (2) The dependence of the Hall signal on the external field is linear between the points marked by "I" and "II" letters. The "I" point corresponds to the field value when the Hall signal begins to decrease from its saturation level; in the "II" point, the abrupt reverse of the magnetization takes place. (3) The "I" point shifts to the higher field with the increase in the irradiation dose from 3×10^{15} and 4×10^{15} ions/cm^2.

Let us now discuss the set of the experimental data. The question we need to answer is "What kind of the magnetization distribution in the round irradiated spots can lead to the radially symmetrical distribution of the MFM signal?" Three thinkable variants are possible (Fig. 3). (1) The formation of the magnetic bubble domain with the reversed magnetization. It can take place in the case when the irradiation slightly reduces the anisotropy value (and, possibly, coercivity) within the spot, but it is still of the easy-axis character. (2) If the irradiation is higher, the effective anisotropy can acquire the easy plain character within the spot. The
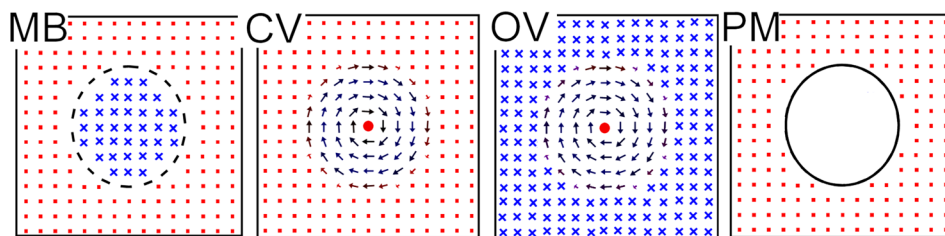
FIG. 3. Possible magnetization configurations within the irradiated spot: MB—magnetic bubble, CV—co-directional vortex (magnetization of the core is codirectional to the film magnetization), OV—opposite vortex (magnetization of the core is opposite to the film magnetization), and PM—paramagnetic state. Points (red) and crosses (blue) denote the magnetic moments directed perpendicular to the film plain in the opposite directions. Dashed circle is the domain wall of the magnetic bubble.

A=2.5x10e-13J/m

magnetization will lie in the plain and will form single domain or vortex state within the round spot similarly to magnetic nanodisks. Evidently, only the vortex will have radially symmetrical MFM signals. Also, there is a 90° domain wall between the vortex located in the spot and surrounding perpendicularly magnetized area. (3) There is also the possibility that the highest irradiation doses can lead to the interlayer mixing of Co and Pt, and the film becomes paramagnetic within the spot.[24]

Evidently, the "vortex" or the paramagnetic spot should demonstrate similar MFM contrast both for the up- and down direction of the magnetization in the surrounding domain. This is similar to the MFM picture observed for the high irradiation doses. In this situation, the formation of the Hall signal hysteresis can help to distinguish between these two cases. Indeed, the remanent magnetization of the system with paramagnetic spots will be equal to saturation. Vice versa if the magnetization in the spots will lie down to form the vortices the remanent magnetization should be less than saturation. According to the geometry of the sample (the 100 nm spots arranged in the square lattice with the period of 200 nm), the remanent magnetization should be 80% of the saturation in the case of the formation of vortices. Exactly the same value is observed in the case of the system with highly irradiated spots. So, we can conclude that the formation of the magnetic vortices within the spots takes place in this case.

We carried out additional numeric simulations (solid lines in Fig. 4) to fit experimental data. We simulate the 400×400 nm part of the film containing 4 spots with the periodical boundary conditions. The procedure of the simulation

is similar to that used in Ref. 20 where it is described in detail. The material parameters for simulation are chosen in such a way as to ensure the best match of the simulation and experiment. The best fit is achieved for $M_s = 2 \times 10^5$ A/m, $K_u = 3.1 \times 10^4$ J/m^3, and $A = 2.5 \times 10^{11}$ J/m (it is the magnetization, initial uniaxial anisotropy, and exchange coefficient, respectively). The anisotropy coefficient in the spot is 1.72×10^4 J/m^3 and 1.39×10^4 J/m^3 (for the dose of 3×10^{15} and 4×10^{15} ions/cm^2). In the case of the vortex formation within the spots, the coincidence between experimental data and numerical calculations is very good. The remanent magnetization is 80%; we also observe the shift of the "I" point in the graph to the larger values of the external field with the decrease in the anisotropy coefficient in the spot in simulation. This corresponds to the expected decrease in the perpendicular anisotropy with the increase in the irradiation dose in the experiment. The differences in the calculated and measured hysteresis curve in the "II – III" branch will be discussed below.

Unfortunately, the used MFM does not allow us to distinguish the core of the vortex and directly distinguish co-directional vortex (C-vortex) and opposite vortex (O-vortex) (Figs. 3(b) and 3(c)). Nevertheless, we should notice the following: The direction of the magnetization of the vortex core should coincide with the magnetization direction in the surrounding nonirradiated area in the remanent state; so, we have the lattice of C-vortices in the remanent state. The observed reversal of the perpendicularly magnetized nonirradiated area of the system takes place at the field ∼100 Oe ("II" point at the Figs. 4(b) and 4(c)). This value is much less than the field which is required to reverse the vortex core
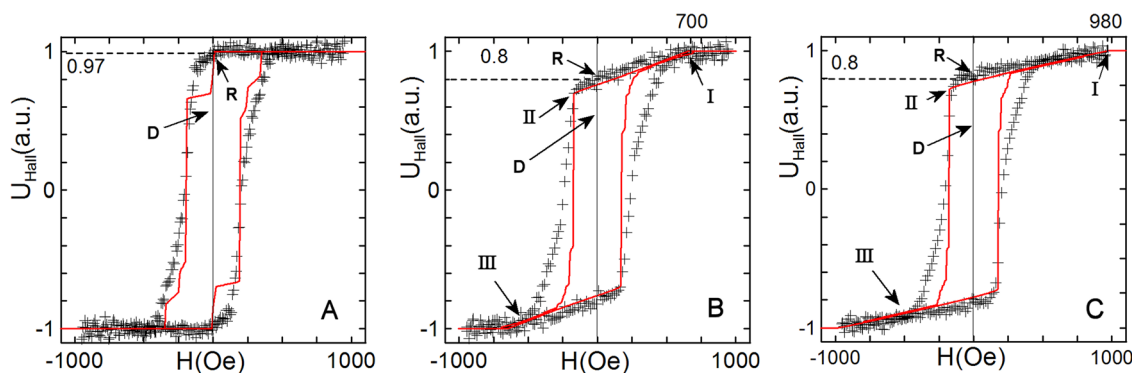

FIG. 4. From the left to the right: normalized Hall effect for the samples with irradiation doses 2×10^{15}, 3×10^{15}, and 4×10^{15} ions/cm^2. Crosses are the experimental data; the solid red line is for numerical simulation. R and D denote the point corresponding to the remanent and demagnetized states; I–II is the range of the linear dependence of the Hall effect on the external field.

polarity.[25] So, first the reversal takes place by the nucleation and propagating of the reversed domains in the nonirradiated area (Fig. 2(b)) while the vortex cores preserve their polarity. It means that the unreversed domains (dark in Fig. 2(b)) surround C-vortices, while reversed domains contain O-vortices (light domain with dark spots in Fig. 2(b)). In the latter case, the magnetization continuously deform from up in the center of the O-vortex to down at the periphery in all radial directions away from the center. Thus, the O-vortex is topologically equal to skyrmions. Vise versa the C-vortex does not have a topological charge.[26] So, the "vortices" acquire the topological charge on the "II"→ "III" branch of the hysteresis curve while the nonirradiated part of the film reverses and C-vortices become O-vortices. The density of the topological charge in the system in this case can be estimated as 25 μm^{-2}. The appearance of the topological charge additionally contributes to the Hall effect. Together with some coercivity fluctuations in the experimental sample which cannot be simulated, this possibly can explain the difference of the experimentally observed and calculated values of the Hall effect at the "II"→"III" branch in Figs. 4(b) and 4(c). Let us notice that the suggested scenario of the reversal is observed in the carried simulation also.

For small irradiation dose, we observe the partially magnetized lattice of the spots (Fig. 2(c)) and the absence of the spot contrast on the background of the reversed domains (Fig. 2(d)). This is possible only in the case of the magnetic bubble domain formation in the spot. Evidently, if the magnetization within the spot is codirectional to the magnetization in the surrounding area, then there is a local uniform magnetization without any local MFM contrast. The topological charge of the magnetic bubbles depends on their domain wall structure which cannot be resolved by MFM. The micromagnetic simulation shows the formation of the Bloch-type bubbles when the anisotropy retains perpendicular character within the spot ($K_{sp} = 2.38 \times 10^4$ J/m^3). The topology of such magnetic bubbles is also identical to the magnetic skyrmion.

The difference between the measured and the calculated curves in Fig. 4(a) corresponding to the magnetic bubble formation in the spots can also be explained by the possible variation of the coercivity from spot to spot. The sharp step in the simulated curve is due to the nearly simultaneous formation of all of the bubbles in the system. This step smoothes if due to coercivity dispersion the bubbles appear one-by-one with the increase in the external field. The more fundamental contradiction which cannot be explained by the coercivity dispersion is the one between the MFM (Fig. 2(c)) and Hall (Fig. 4(a)) experimental data related to this sample. Indeed, the MFM measurements demonstrate the formation of the bubbles in the 75% of the spots in the lattice at the zero external field. According to the geometry of the sample, the remanent magnetization should be 70% of the saturation in this case. At the same time, the measured Hall signal corresponding to this state is as high as 97%. Such difference is observed only for the sample with the magnetic bubble formation; the samples with the vortices demonstrate good correlation of MFM picture and Hall signal in the remanent state. Whereas the C-vortices which are formed in the remanent state of the highly irradiated spots are topologically

uncharged, the magnetic bubbles can carry some topological charge depending on their domain wall structure. As the density of the magnetic bubbles is high enough, there can be additional topological contribution to the Hall effect in this case. This addition can lead to the difference in the observed (97% of saturation) and expected (70%) values of the Hall signal in the remanence. We do not claim the observation of the topological Hall effect here, but we point out that this can be one of the possible explanations of the abnormal values of the measured Hall signal in the discussed systems.

In conclusion, we used the focused ion beam technology to change the value of the anisotropy of the Co/Pt multilayers locally. MFM measurements show that depending on the dose, either the magnetic bubbles or magnetic vortices are formed in the irradiated spot. In the case when the vortex core within the spot is oppositely directed to the magnetization of nonirradiated area, the spin texture is identical to the magnetic skyrmion. The density of the topological charge in the system can be estimated as 25 μm^{-2} in this case. Additional investigations are needed to verify if the noticeable topological Hall effect takes place in the system. Let us also notice that in principle, interfacial DMI is possible in the Co/Pt multilayers.[27] The observation of the labyrinth domain structure in the nonirradiated film demonstrates that DMI is not enough to form and stabilize localized topologically charged states in the as-prepared film. Nevertheless, the local modification of the anisotropy makes it possible to stabilize the skyrmion-lake states in the system.

[1]I. E. Dzyaloshinskii and B. A. Ivanov, JETP Lett. **29**, 540 (1979).
[2]A. S. Kovalev, A. M. Kosevich, and K. V. Maslov, JETP Lett. **30**, 296 (1979).
[3]S. Muhlbauer, B. Binz, F. Jonietz, C. Pfleiderer, A. Rosch, A. Neubauer, R. Georgii, and P. Boni, Science **323**, 915 (2009).
[4]X. Z. Yu, Y. Onose, N. Kanazawa, J. H. Park, J. H. Han, Y. Matsui, N. Nagaosa, and Y. Tokura, Nature (London) **465**, 901 (2010).
[5]S. Heinze, K. von Bergmann, M. Menze, J. Brede, A. Kubetzka, R. Wiesendanger, G. Bihlmayer, and S. Blugel, Nat. Phys. **7**, 713 (2011).
[6]U. K. Rossler, N. Bogdanov, and C. Pleiderer, Nature (London) **442**, 797 (2006).
[7]Y. Onose, N. Takeshita, C. Terakura, H. Takagi, and Y. Tokura, Phys. Rev. B **72**, 224431 (2005).
[8]A. Neubauer, C. Pfleiderer, B. Binz, A. Rosch, R. Ritz, P. G. Niklowitz, and P. Boni, Phys. Rev. Lett. **102**, 186602 (2009).
[9]F. Jonietz, S. Muhlbauer, C. Pfleiderer, A. Neubauer, W. Munzer, A. Bauer, T. Adams, R. Georgii, P. Boni, R. A. Duine, K. Everschor, M. Garst, and A. Rosch, Science **330**, 1648 (2010).
[10]A. Bogdanov and A. Hubert, J. Magn. Magn. Mater. **138**, 255 (1994).
[11]A. Bogdanov and A. Hubert, J. Magn. Magn. Mater. **195**, 182 (1999).
[12]H. Y. Kwon, K. M. Bu, Y. Z. Wu, and C. Won, J. Magn. Magn. Mater. **324**, 2171 (2012).

[13]N. Nagaosa and Y. Tokura, Nat. Nanotechnol. **8**, 899 (2013).

[14]L. Sun, R. X. Cao, B. F. Miao, Z. Feng, B. You, D. Wu, W. Zhang, An. Hu, and H. F. Ding, Phys. Rev. Lett. **110**, 167201 (2013).

[15]K. Xie and H. Sang, J. Appl. Phys. **116**, 223901 (2014).

[16]B. F. Miao, L. Sun, Y. W. Wu, X. D. Tao, X. Xiong, Y. Wen, R. X. Cao, P. Wang, D. Wu, Q. F. Zhan, B. You, J. Du, R. W. Li, and H. F. Ding, Phys. Rev. B **90**, 174411 (2014).

[17]J. Li, A. Tan, K. W. Moon, A. Doran, M. A. Marcus, A. T. Young, E. Arenholz, S. Ma, R. F. Yang, C. Hwang, and Z. Q. Qiu, Nat. Commun. **5**, 4704 (2014).

[18]A. A. Fraerman, O. L. Ermolaeva, E. V. Skorohodov, N. S. Gusev, V. L. Mironov, S. N. Vdovichev, and E. S. Demidov, J. Magn. Magn. Mater. **393**, 452 (2015).

[19]M. V. Sapozhnikov and O. L. Ermolaeva, Phys. Rev. B **91**, 024418 (2015).

[20]M. V. Sapozhnikov, J. Magn. Magn. Mater. **396**, 338 (2015).

[21]C. Chappert, H. Bernas, J. Ferre, V. Kottler, J.-P. Jamet, Y. Chen, E. Cambril, T. Devolder, F. Rousseaux, V. Mathet, and H. Launois, Science **280**, 1919 (1998).

[22]T. Devolder, J. Ferre, C. Chappert, H. Bernas, J.-P. Jamet, and V. Mathet, Phys. Rev. B **64**, 064415 (2001).

[23]A. Aziz, S. J. Bending, H. Roberts, S. Crampin, P. J. Heard, and C. H. Marrows, J. Appl. Phys. **99**, 08C504 (2006).

[24]E. Suharyadi, D. Oshima, T. Kato, and S. Iwata, Results Phys. **6**, 186 (2016).

[25]T. Okunoa, K. Shigetoa, T. Onob, K. Mibua, and T. Shinjo, J. Magn. Magn. Mater. **240**, 1 (2002).

[26]A. M. Kosevich, B. A. Ivanov, and A. S. Kovalev, Physica D **3**, 363 (1981).

[27]H. Yang, A. Thiaville, S. Rohart, A. Fert, and M. Chshiev, Phys. Rev. Lett. **115**, 267210 (2015).